Available online at www.sciencedirect.com
SCIENCE DIRECT®
Journal of Nuclear Materials 329–333 (2004) 899–903
journal of nuclear materials
www.elsevier.com/locate/jnucmat

Energetic deuterium and helium irradiation effects on chemical structure of CVD diamond

M. Sasaki [a,*], Y. Morimoto [a], H. Kimura [a], K. Takahashi [b], K. Sakamoto [b], T. Imai [b], K. Okuno [a]

[a] *Faculty of Science, Radiochemistry Research Laboratory, Shizuoka University, 836 Oya, Shizuoka-shi, Shizuoka 422-8529, Japan*
[b] *Naka Fusion Research Establishment, Japan Atomic Energy Research Institute, 801-1, Naka-machi, Ibaraki 311-0193, Japan*

Abstract

The effects of energetic deuterium and helium irradiation on the chemical structure of CVD diamond and the existing states of the deuterium were investigated by means of the XPS technique. The variations of C1s XPS spectra indicated a change of diamond structure under both ion irradiations. The C1s chemical shift of D_2^+ irradiation was smaller than that of He^+ irradiation, and the chemical shift was −0.6 and −2.5 eV, respectively. The variation of the C1s FWHM of D_2^+ irradiation was also smaller than that of He^+ irradiation, and the FWHM was 0.1 and 0.7 eV, respectively. This difference in the chemical shift and FWHM could be explained by the formation of C–D bond between carbon atoms and the trapped deuterium atoms.

1. Introduction

A radio frequency (RF) heating system is a promising candidate for plasma heating and plasma current drive in future fusion reactors [1]. In particular, the electron cyclotron range of frequencies (ECRF) is very attractive for electron cyclotron heating and current drive (ECH/ECCD) in an experimental fusion device such as ITER. The ECH/ECCD system consists of a RF source (gyrotron), a RF transmission line, and an antenna to inject the RF power into plasma. The output window of the gyrotron and the transmission line are two of the most important components in the ECH/ECCD system [2,3]. The window materials should have low dielectric loss and high thermal conductivity for the purpose of high power (∼1 MW) and continuous wave transmission. CVD diamond has properties that satisfy the above conditions; low loss tangent in the ECRF and five times higher thermal conductivity than copper. Large size polycrystalline diamond disks have been manufactured by chemical vapor deposition (CVD) technology for several years and are available for the RF window.

A D–T burning fusion reactor contains radioactive and hazardous materials such as tritium, neutron activation products, dust from reactor operation, etc. The diamond window used in the transmission line, which is called a torus window, is located far from the plasma to reduce direct exposure to energetic particles. However, it is still exposed to energetic and/or thermal deuterium, tritium and helium, and radioactive dust. The particles, such deuterium and tritium, have strong chemical affinities for carbon. Therefore, it is an important safety issue in the ECH/ECCD system to elucidate the effects of particle exposure on structure changes in the diamond window.

In the present study, structure change and chemical bonding with implanted ions in the CVD diamonds were investigated by X-ray Photoelectron Spectroscopy (XPS) after energetic ion irradiation. By comparing experimental results after deuterium ion irradiation with those after helium irradiation, we will discuss the chemical and physical influences of ion irradiations on the diamond structure.

* Corresponding author. Tel.: +81-54 238 6436; fax: +81-54 238 3989.
E-mail address: r0232010@ipc.shizuoka.ac.jp (M. Sasaki).

0022-3115/$ - see front matter © 2004 Elsevier B.V. All rights reserved.
doi:10.1016/j.jnucmat.2004.04.275

2. Experimental

Polycrystalline diamond disks produced by CVD were purchased from Element Six Ltd. Co. They were same grade as the diamond window of a 170 GHz high power gyrotron that has been developed for ITER [3]. Their dimensions were 10 mm in diameter and 0.2 mm in thickness.

XPS measurements were carried out at room temperature using an X-ray photoelectron spectrometer (ULVAC-PHI INC. ESCA1600). The detail of the apparatus was described in Ref. [4]. The chamber of the apparatus was evacuated to a pressure of 10^{-8} Pa. Aluminum Kα radiation with a photon energy of 1486.6 eV was used as the light source. The emitted photoelectrons were collected in the Concentric Hemispherical Analyzer with pass energy of 46.95 and 187.85 eV for the narrow-energy-range of C1s and valence band, and the wide-energy-range, respectively.

The condition of an as-received sample was analyzed by XPS and the XPS wide-range spectrum indicated that there were oxygen atoms as an impurity. After removing surface oxygen impurity by heating at 823 K for 10 min under ultrahigh vacuum (below $\sim 5\times10^{-8}$ Pa), the diamond disk was used as sample.

2.1. Ion fluence dependence

After the heat treatment, the sample was analyzed by measuring the narrow-energy-range C1s and valence band spectrum with XPS. Then, the deuterium (D_2^+) or helium (He^+) ions were implanted into the sample with the flux of 1.2×10^{18} D^+ $m^{-2}\,s^{-1}$ or 8.1×10^{17} He^+ $m^{-2}\,s^{-1}$ at the surface normal. The irradiation energies of D_2^+ and He^+ were 0.25 keV D^+ and 0.45 keV He^+, respectively, which were chosen so both ions would have the same ion range, 3.5 nm which is considerably larger than the escape depth of photoelectron. After the ion irradiations, the XPS spectra were measured in situ. The D_2^+ or He^+ irradiation and XPS measurements were repeated sequentially up to the ion fluence up to 1.3×10^{22} m^{-2}.

2.2. Thermal annealing after ion irradiation

A sample pretreated by heating was analyzed by measuring the narrow-energy-range C1s and valence band spectrum with XPS. Then, the 0.5 keV D_2^+ or 0.45 keV He^+ were implanted into the sample with the ion flux of 1.0×10^{18} D^+ $m^{-2}\,s^{-1}$ or 5.6×10^{17} He^+ $m^{-2}\,s^{-1}$ at the surface normal. The ion irradiation was carried out to the ion fluence of 1.5×10^{22} m^{-2}. The sample irradiated with ions was heated for 10 min stepwise intervals with a temperature increment of 175 or 200 K up to 1373 K, and desorped gases were analyzed with QMS. After each heating, the diamond structure was measured by XPS.

3. Results

Fig. 1 shows the XPS spectra of the pretreated sample and isotropic graphite (as a reference), respectively. From Fig. 1, the C1s peak of the diamond was at 288.5 eV and its full width at half maximum (FWHM) was 1.6 eV. The peak position and the FWHM of the isotropic graphite C1s peak were 284.4 and 1.3 eV, respectively. The XPS spectrum of the isotropic graphite showed a π–π^* transition resulting, at approximately +6 eV above the C1s binding energy [5,6]. This π–π^* transition was never observed for the pretreated diamond sample.

3.1. Ion fluence dependence

Fig. 2 shows the dependence of the C1s chemical shift, FWHM, and $sp^3/(sp^3+sp^2)$ on the He^+ fluence, where $sp^3/(sp^3+sp^2)$ was a ratio of the total amount of peak area of C2p to the amount of peak area of C2p (sp^3) in the valence band XPS spectra. The C1s peak shifted toward lower energy with increasing He^+ fluence up to 0.5×10^{22} He^+ m^{-2}, and the chemical shift finally reached was −2.5 eV. The FWHM decreased up to 0.1×10^{22} He^+ m^{-2}, and after that increased up to 0.5×10^{22} He^+ m^{-2}. The FWHM changed with the He^+ fluence from 1.6 to 2.3 eV. The valence band structure was identified from Ref. [7]. The peaks observed at ~23, ~17, ~12 and ~8 eV were identified with photoelectrons emitted from the O2s, C2s, C2p (sp^3) and C2p (sp^2) levels, respectively. It can be seen from Fig. 2 that the $sp^3/(sp^2+sp^3)$ ratio decreased with increasing He^+ fluence up to 0.6×10^{22} He^+ m^{-2}.

Fig. 3 shows the dependence of the C1s chemical shift, FWHM, and the sp^3 to (sp^3+sp^2) ratio on the D^+ fluence. The C1s peak shifted toward lower energy with

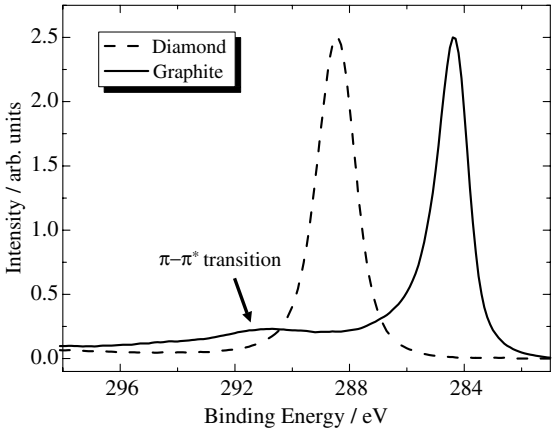

Fig. 1. The XPS C1s peaks of the pretreated sample and isotropic graphite. The solid and dotted lines indicate the diamond sample and isotropic graphite, respectively.

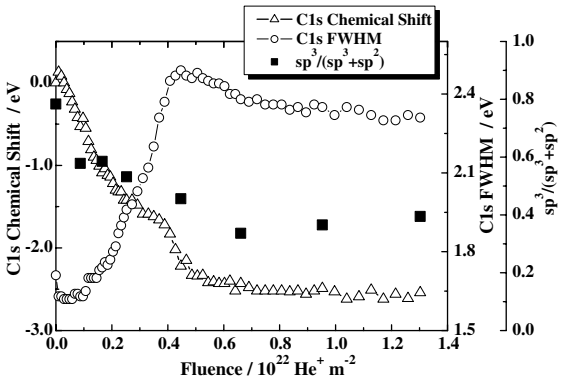

Fig. 2. The dependence of the C1s chemical shift, FWHM and $sp^3/(sp^3 + sp^2)$ on the He^+ fluence. The triangle, circle and solid square indicate the C1s chemical shit, FWHM and $sp^3/(sp^3 + sp^2)$, respectively. '$sp^3/(sp^3 + sp^2)$' was a ratio of the total amount of peak area of C2p to the amount of peak area of C2p (sp^3) in the valence band XPS spectra.

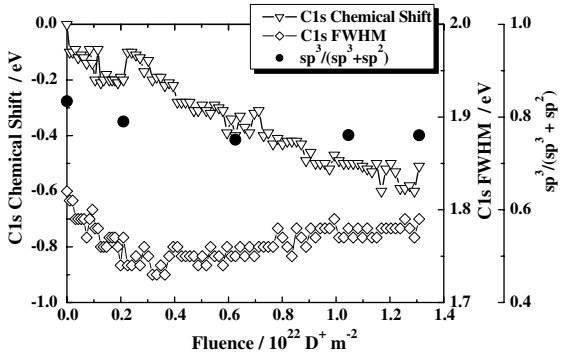

Fig. 3. The dependence of the C1s chemical shift, FWHM and $sp^3/(sp^3 + sp^2)$ on the D^+ fluence. The inverted triangle, diamond and solid circle indicate the C1s chemical shit, FWHM and $sp^3/(sp^3 + sp^2)$, respectively. '$sp^3/(sp^3 + sp^2)$' was a ratio of the total amount of peak area of C2p to the amount of peak area of C2p (sp^3) in the valence band XPS spectra.

increasing D^+ fluence up to 1.0×10^{22} D^+ m^{-2}, and the chemical shift finally reached was −0.6 eV. The FWHM decreased up to 0.3×10^{22} D^+ m^{-2} and after that increased up to 1.0×10^{22} D^+ m^{-2}. The FWHM changed with the D^+ fluence from 1.7 to 1.8 eV. The $sp^3/(sp^3 + sp^2)$ ratio was constant practically, independent of the D_2^+ fluence.

3.2. Thermal annealing after ion irradiation

Fig. 4(a) shows the dependence of the C1s XPS spectra on heating temperature after the He^+ irradiation. The C1s peak remained at the almost the same binding energy, 284.4 eV, after each heating increment which is consistent with that for the isotropic graphite

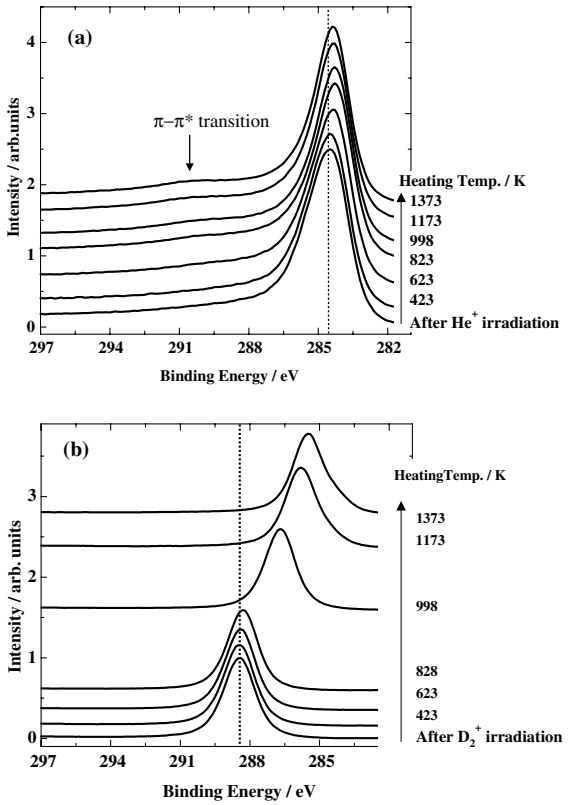

Fig. 4. The dependence of the C1s XPS spectra on heating temperature after (a) the He^+ irradiation and (b) the D_2^+ irradiation.

sample. The π–π* transition became clear with increasing the heating temperature. On the other hand, the FWHM of the C1s peak became gradually narrower with increasing the heating temperature.

Fig. 4(b) shows the dependence of the C1s XPS spectra on heating temperature after the D_2^+ irradiation. The C1s peak energy began to shift toward lower energy at 800 K. After heating at 1373 K, the C1s peak reached 285.4 eV, which was higher than that for isotropic graphite. The π–π* transition was never observed in the C1s spectra.

Fig. 5 shows the dependence of the C1s chemical shift for sample irradiated with 0.25 keV D^+ and no-irradiated sample and D_2 gas release ratio on heating temperature. The D_2 gas release ratio was defined as the ratio of the total amount of released D_2 gas to the amount of released D_2 gas at the indicated heating temperature. The C1s peak energy of the no-irradiated sample began to shift toward lower energy around 700 K, and the chemical shift finally reached was −3.4 eV. The FWHM and $sp^3/(sp^3 + sp^2)$ ratio were increased by only heat treatment. The C1s peak energy of the sample irradiated with 0.25 keV D^+ began to shift toward lower

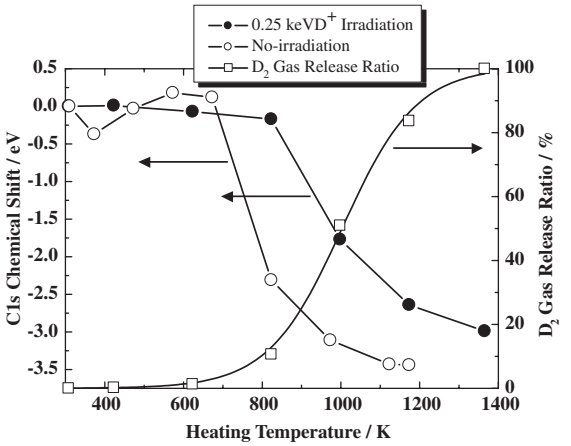

Fig. 5. The dependence of the C1s chemical shift for sample irradiated with 0.25 keV D^+ and no-irradiated sample and D_2 gas release ratio on heating temperature. The solid circle, circle and square indicate the C1s chemical shit of irradiated sample with 0.25 keV D^+ and no-irradiated sample and D_2 gas release ratio, respectively.

energy at 800 K, and the chemical shift finally reached was −3.0 eV. The D_2 gas also began to release at 800 K.

4. Discussion

4.1. Ion fluence dependence

After both He^+ and D_2^+ irradiation, the shift to lower energy and the increase of the FWHM of the C1s peak were observed. The energy shift could be attributed to irradiation damage such as lattice displacements [8,9]. The increase of the FWHM was due to the presence of more than one bonding phase. These results indicate that the diamond structure became disordered state due to the ion irradiation. That is, carbon atoms in the diamond received sufficient energy from energetic ions to disorder the diamond structure. Then, it is expected that the energy would be also used for relaxation of the sp^3 bonds of the carbon atom to sp^2 bonds because diamond structure is less stable thermodynamically than graphite (the free energy of formation of diamond is 2.90 kJ mol^{-1} greater than graphite) [6]. The disordering and relaxation of the diamond structure occurred simultaneously and eventually achieved the equilibrium state during the ion irradiation. Finally, the diamond structure became disordered state, in which sp^3 bonds and sp^2 bonds coexisted.

In the case of the He^+ irradiation, the $sp^3/(sp^3 + sp^2)$ ratio decreased, as shown in Fig. 2. This indicates that the sp^3 bonds were practically all changed into sp^2 bonds by irradiation with energetic He^+ as supposed above.

Comparison of the results with D_2^+ irradiation with that for He^+, it was found that there were differences in the C1s and valence band in XPS spectra. As shown in Figs. 2 and 3, the C1s chemical shift in the D_2^+ irradiation was smaller than that in the He^+ irradiation. In other words, the C1s peaks in the D_2^+ irradiation were located at higher energy than that in the He^+ irradiation. This indicates that C–D bond formation between carbon atoms and the trapped deuterium atoms was induced by D_2^+ irradiation because the formation of C–D bond results in a decrease in the electron population of carbon atom, and also an increase of the binding energy of the C1s level [6,9,10]. In addition, the $sp^3/(sp^3 + sp^2)$ ratio was almost constant. This indicated that the sp^3 bonds remained during the D_2^+ irradiation. In the case of the D_2^+ irradiation, the irradiated D_2^+ combined with carbon atoms, and the sp^3 bonds were kept by the deuterium atoms, that is, the deuterium atoms terminated carbon atoms with an sp^3 hybrid orbital. The C–D bonds prevented the conversion from the sp^3 bonds to sp^2 bonds.

4.2. Thermal annealing after ion irradiation

After the He^+ irradiation, the sp^2 bond was dominant rather than the sp^3 bonds. In Fig. 4(a), the π–π^* transition was not observed in the C1s XPS spectrum after the He^+ irradiation. This indicates that the graphite network would not develop in the sample. After sample heating, the π–π^* transition became clear in the C1s XPS spectra. The sp^3 bonds, which remained after the He^+ irradiation, converted to the sp^2 bonds. As a result, the graphite network was extended by the converted sp^2 bonds.

On the other hand, in the case of the D_2^+ irradiation, no π–π^* transition was observed even after annealing. This indicated that the graphite network was not developing in the area irradiated by D_2^+ after heating sample. In the case of the no-irradiated sample, the π–π^* transition was not observed similarly. After annealing sample irradiated with He^+, π–π^* transition was observed. This difference revealed that graphite network was developed by a combination of irradiation damage and heat.

The chemical shift toward lower energy of the sample irradiated with D_2^+ caused by release of D_2 gases from the sample and conversion of sp^3 to sp^2. By heating the sample, the C–D bond was broken and sp^2 bond was formed. In the case of no-irradiated sample, the chemical shift was observed at lower temperature than that of the sample irradiated with D_2^+. This difference revealed that the trapped deuterium atom prevented the sp^3 bonds from converting to sp^2 bonds.

5. Conclusion

The effects of energetic deuterium and helium irradiation on the chemical structure of CVD diamond and

the existing states of the deuterium were investigated by means of the XPS technique.

The C1s XPS spectra were dramatically changed when 0.45 keV He^+ was implanted into the sample. This confirmed that He^+ irradiation changed most sp^3 bonds to sp^2 bonds, resulting in a disordered state, which is an incipient or undeveloped graphite network. Thermal annealing after the He^+ irradiation accelerated the development of the graphite network.

However, the XPS spectra were hardly changed when 0.5 keV D_2^+ was implanted into the sample. Comparison of the XPS results of the deuterium with that of the helium revealed C–D bond formation between carbon atoms with an sp^3 hybrid orbital and the trapped deuterium atoms. The heating subsequent treatment caused conversion of the sp^3 bonds into sp^2 bonds followed by deuterium being released from the sample. However, the graphite network did not develop. It is possible that the C–D bonds prevented graphitizing in the D_2^+ implanted area.

References

[1] M. Makowski, IEEE Trans. Plasma Sci. 24 (1996) 1023.
[2] O. Braz, A. Kasugai, K. Sakamoto, K. Takahashi, M. Tuneoka, T. Imai, M. Thumm, Int. J. Infrared Millim. Waves 18 (1997) 1945.
[3] K. Sakamoto, A. Kasugai, M. Tuneoka, K. Takahashi, T. Imai, T. Kariya, Y. Mitsunaka, Rev. Sci. Instrum. 70 (1999) 208.
[4] Y. Morimoto, T. Sugiyama, S. Akahori, H. Kodama, E. Tega, M. Sasaki, M. Oyaidu, H. Kimura, K. Okuno, Phys. Scr. T103 (2003) 117.
[5] F.R. Mc Feeley, S.P. Kowalczyk, L. Ley, R.G. Cavell, R.A. Pollak, D.A. Shirley, Phys. Rev. B 9 (1974) 5268.
[6] V.S. Smentkowski, H. Jänsch, M.A. Henderson, J.T. Yates Jr., Surf. Sci. 330 (1995) 207.
[7] J.I.B. Willson, J.S. Walton, G. Beamson, J. Electron. Spectrosc. Relat. Phenom. 121 (2001) 183.
[8] Y. Morimoto, M. Sasaki, H. Kimura, K. Sakamoto, T. Imai, K. Okuno, Fusion Eng. Des. 66–68 (2003) 651.
[9] Y. Gotoh, O. Okada, J. Nucl. Sci. Technol. 21 (1984) 205.
[10] G. Francz, P. Oelhafen, Surf. Sci. 329 (1995) 193.